

Supplemental Information for

Molecular Basis for the Activation of a Catalytic Asparagine Residue in a Self-Cleaving Bacterial Autotransporter

Travis J. Barnard¹, James Gumbart³, Janine H. Peterson², Nicholas Noinaj¹,
Nicole C. Easley¹, Nathalie Dautin², Adam J. Kuszak¹, Emad Tajkhorshid⁴,
Harris D. Bernstein², Susan K. Buchanan¹

¹Laboratory of Molecular Biology

²Genetics and Biochemistry Branch

National Institute of Diabetes and Digestive and Kidney Diseases, US National
Institutes of Health, Bethesda, Maryland 20892

³Biosciences Division, Argonne National Laboratory, Argonne, Illinois 60439

⁴Center for Biophysics and Computational Biology, Department of Biochemistry,
College of Medicine, Beckman Institute for Advanced Science and Technology,
University of Illinois at Urbana-Champaign, Urbana, Illinois 61801

*Correspondence: Susan Buchanan, skbuchan@helix.nih.gov; phone 1-301-594-
9222; fax 1- 301-480-0597; address Susan Buchanan, 50 South Drive, Building
50 Room 4503, Bethesda, MD 20892

Present address: Nathalie Dautin, Department of Biology, The Catholic University
of America, Washington, DC, 20064, USA

Supplemental Figures S1-S5
Supplemental Experimental Procedures
Supplemental References

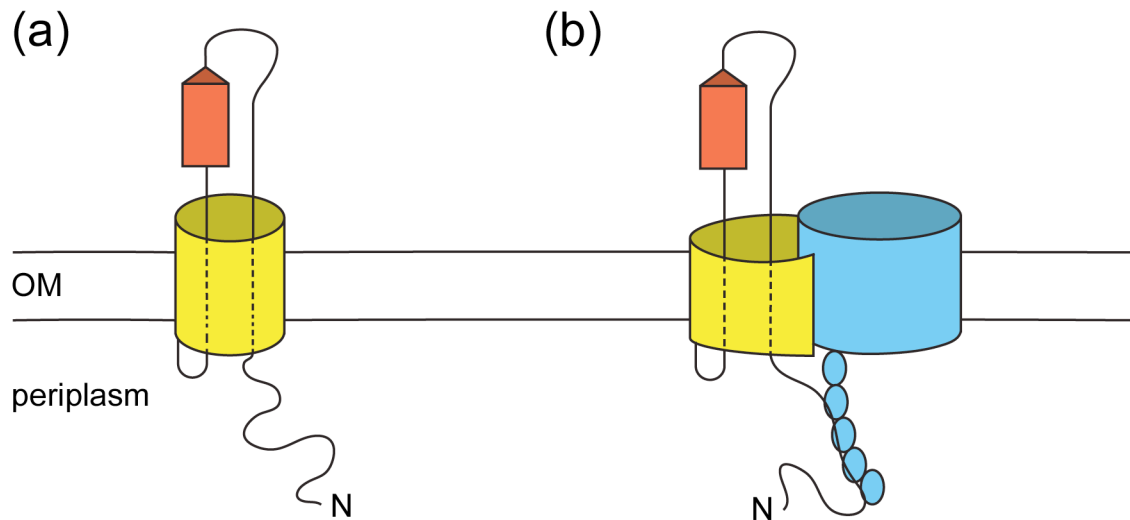


Figure S1. Translocation models. Autotransporter β -domain (yellow), folded passenger domain (red), unfolded passenger (solid or dashed black line), BamA (blue). The N-terminus of the passenger is indicated (N). (a) Hairpin model. (b) BamA model. In both models a hairpin is formed by the C-terminus of the passenger domain. The tip of the hairpin protrudes into the extracellular space while the N-terminal portion of the passenger is still in the periplasm. Folding at the tip of the hairpin provides the energy to pull the passenger from the periplasm to the extracellular space. The primary difference between these models is the pore the passenger passes through to cross the outer membrane. For the Hairpin model, the passenger domain passes through the pore of its β -domain; for the BamA model, the passenger domain passes through a pore created by its partially folded β -domain and the Bam complex (only BamA is shown above). For a more complete description of these models please refer to Oomen *et al.*¹ and Ieva *et al.*².

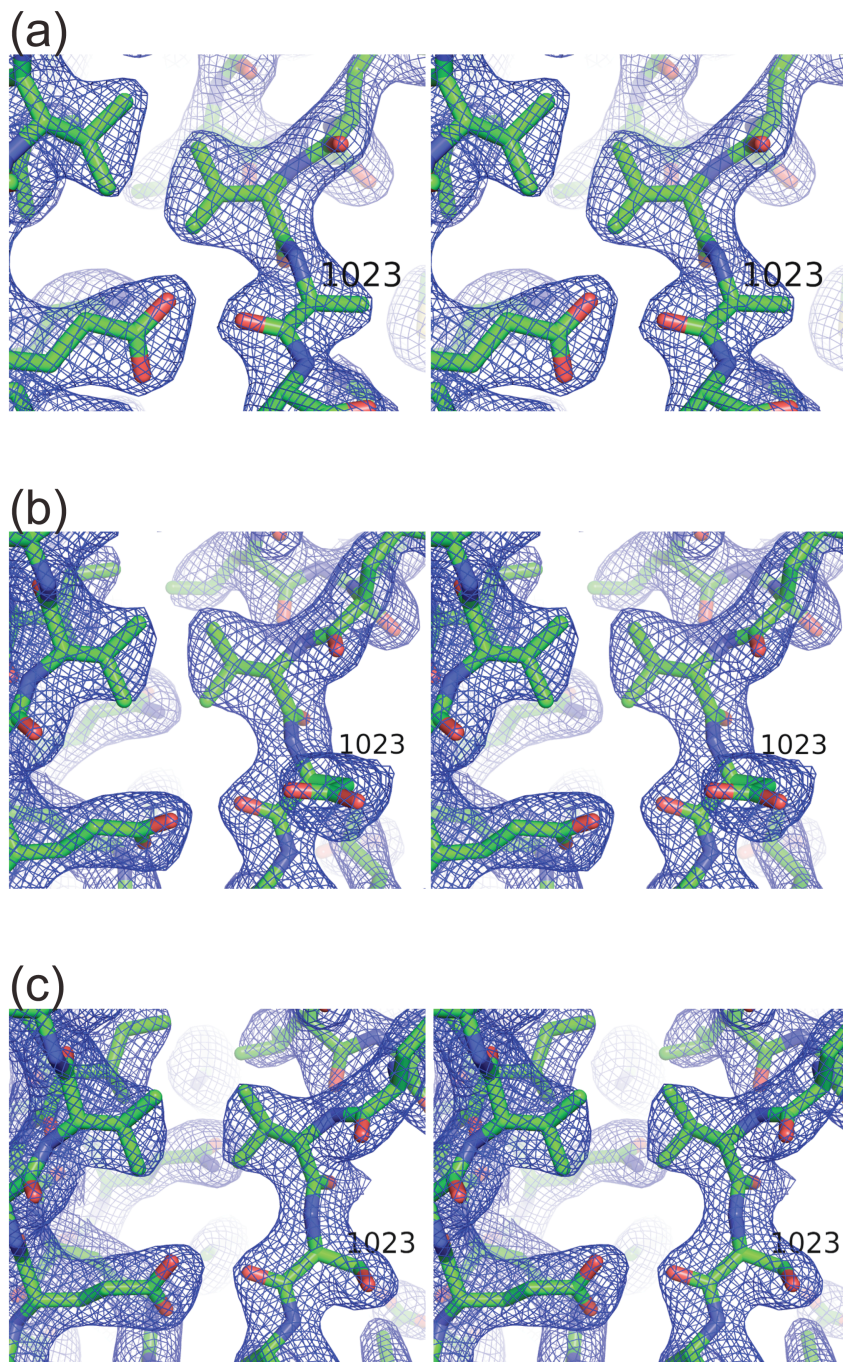


Figure S2. Stereo image of the $(2F_o - F_c)$ electron density map near the cleavage site. (a) N1023A (b) N1023D (c) N1023S. The map is contoured at 1.0σ and position 1023 is labeled.

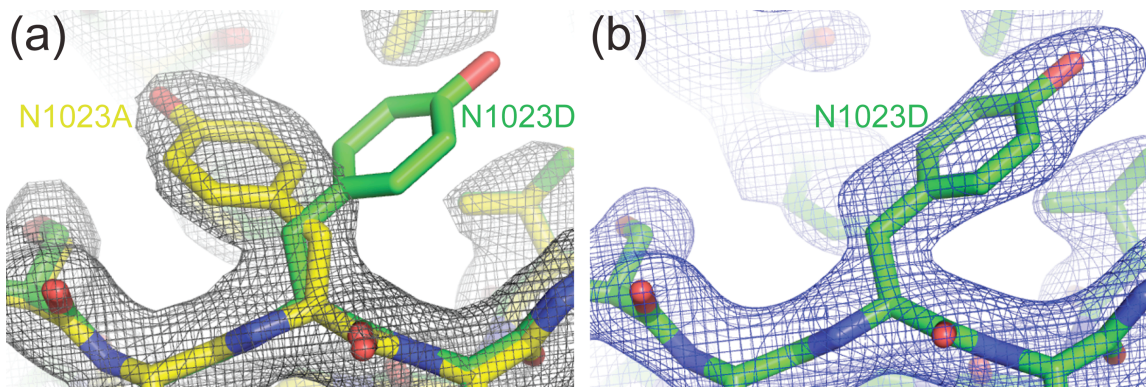


Figure S3. Electron density maps of Tyr1150 in the EspP N1023A (yellow) and N1023D (green) mutants. The map is contoured at 1.0σ . Tyr1150 favors two different conformations that depend on the amino acid substitution at the active site asparagine. For the N1023D mutant, Tyr1150 points towards the cleavage site. For the N1023A mutant, it points away from the cleavage site. (a) The N1023A and N1023D mutants are superposed. The $(2F_o - F_c)$ electron density map for the N1023A mutant is shown. (b) The N1023D mutant alone and its $(2F_o - F_c)$ electron density map.

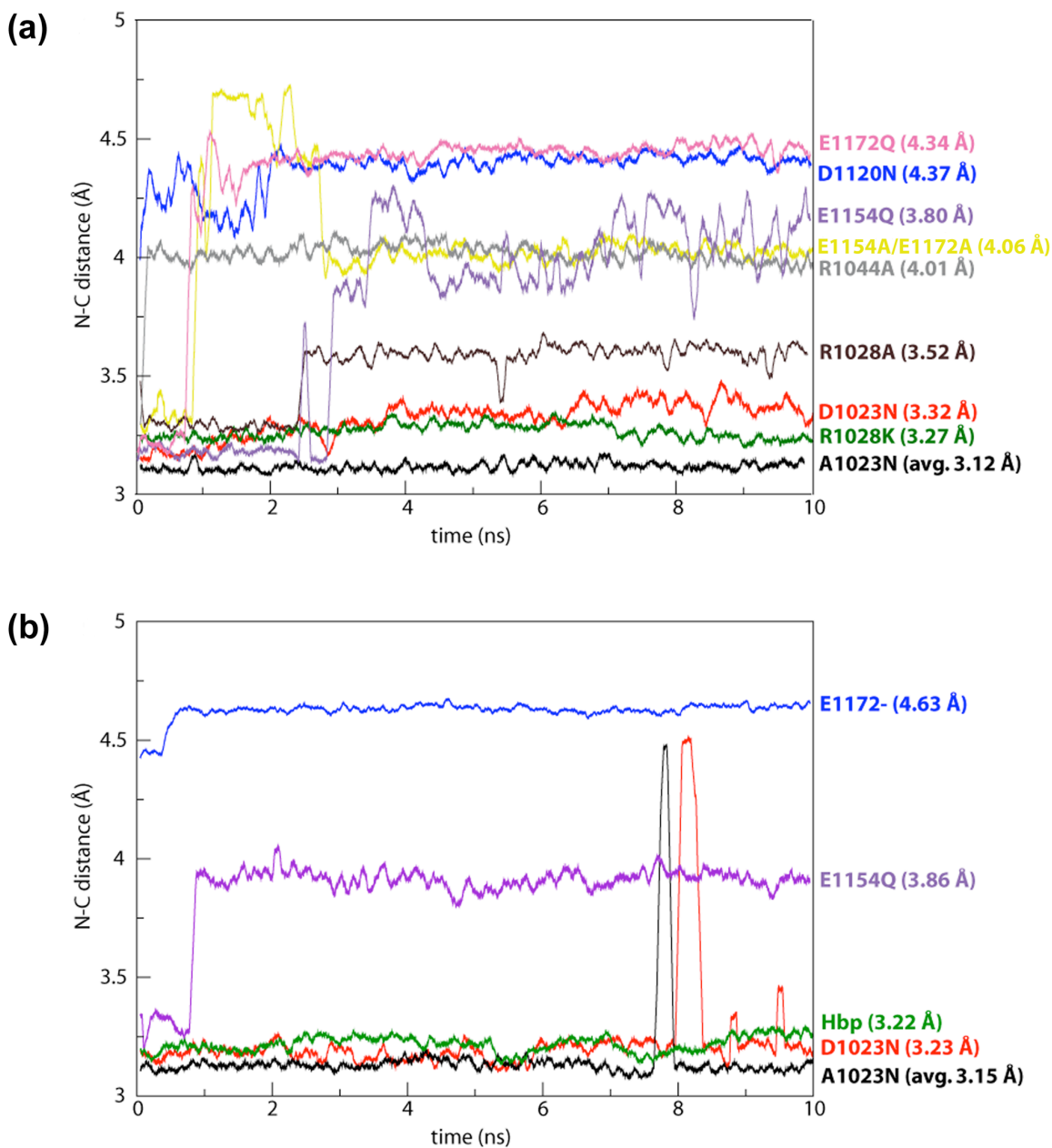


Figure S4. Distance between EspP $N_{\delta}^{Asn1023}$ and $C_{Carb}^{Asn1023}$ (N-C distance) or the equivalent atoms in Hbp in 10 ns molecular dynamics simulations. The average N-C distance is shown in parenthesis. (a) Wild-type EspP and selected EspP mutants. The simulations were performed for wild-type EspP by substituting asparagine at position 1023 of the EspP N1023A or N1023D pre-cleavage structures. These wild-type models are referred to as A1023N and D1023N, respectively. Several EspP mutants that affect cleavage *in vivo* were then simulated in the D1023N background. (b) Repeated runs for the wild-type EspP models A1023N and D1023N, the EspP E1154Q mutant in the D1023N background, and EspP with unprotonated Glu1172 (E1172-) in the D1023N

background. A wild-type model of Hbp was also simulated by replacing the mutant aspartate with the native asparagine at position 1100.

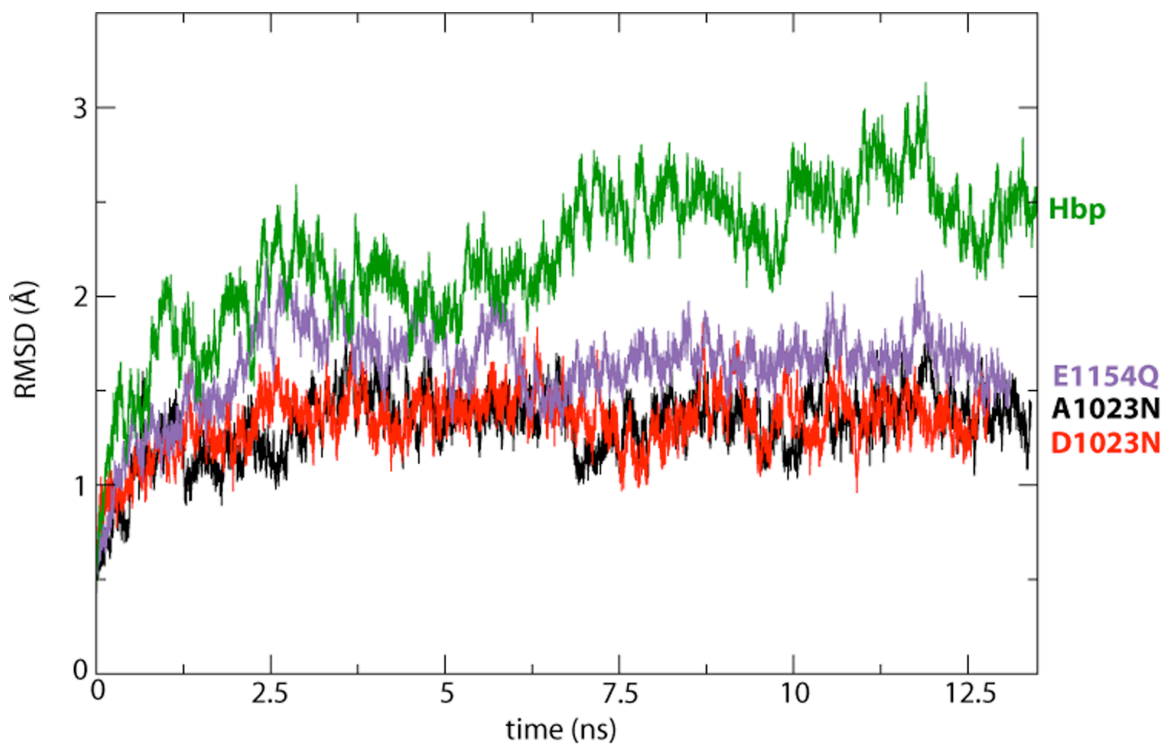


Figure S5. Root mean-square deviation (RMSD) of the protein backbone for selected simulations. Included for each curve are the initial 3.5 ns of equilibration with Asn1023 restrained for EspP or Asn1100 restrained for Hbp followed by the subsequent 10 ns of free simulation. The EspP models A1023N, D1023N, and E1154Q are shown along with the Hbp wild-type model.

Supplemental Experimental Procedures

Expression, purification, and crystallization

The genes used to express the EspP pre-cleavage mutants (N1023A, N1023S, and N1023D) were made by gene synthesis (Biobasic Inc.). The genes were cloned into the EcoRI and HindIII sites of pTrc99a³. Each gene contains the OmpA signal sequence followed by a short linker (APKDN) and six histidines. Directly after the histidine tag, the EspP sequence begins with Ala999.

The EspP pre-cleavage mutants were grown to saturation in Overnight ExpressTM Instant TB Medium (Novagen) containing 100 µg/ml carbenicillin at 37 °C with shaking. The cells were harvested, lysed, and EspP was purified as described previously⁴ with the following exceptions. For the size exclusion step, the column was equilibrated with buffer containing 20 mM Tris HCl pH 7.5, 200 mM NaCl, 0.5 mM EDTA, 0.02% (w/v) Sodium Azide, 0.05% lauryldimethylamine-N-oxide (Fluka), and 0.45% (w/v) tetraethylene glycol monoethyl ether (Anatrace). The purified protein was concentrated to 10 mg/ml. Heptanetriol (Sigma) was added to the protein to a final concentration of 3.0% (w/v) and this protein solution was used for crystallization.

Crystals were grown at 21 °C in hanging drops. The best crystals were grown for the EspP N1023A and N1023S mutants by mixing equal volumes of protein and well solution containing 20% (w/v) PEG 8,000 and 20% (v/v) glycerol. For the EspP N1023D mutant, the best crystals were grown similarly using a well solution containing 18% (w/v) PEG 8,000, 20% (v/v) glycerol, and 25 mM sodium acetate. Crystals were frozen and stored in liquid nitrogen.

Supplemental References

1. Oomen, C. J., van Ulsen, P., van Gelder, P., Feijen, M., Tommassen, J. & Gros, P. (2004). Structure of the translocator domain of a bacterial autotransporter. *EMBO J* **23**, 1257-66.
2. Ieva, R., Tian, P., Peterson, J. H. & Bernstein, H. D. (2011). PNAS Plus: Sequential and spatially restricted interactions of assembly factors with an autotransporter {beta} domain. *Proc Natl Acad Sci U S A*.
3. Amann, E., Ochs, B. & Abel, K. J. (1988). Tightly regulated tac promoter vectors useful for the expression of unfused and fused proteins in *Escherichia coli*. *Gene* **69**, 301-15.
4. Barnard, T. J., Dautin, N., Lukacik, P., Bernstein, H. D. & Buchanan, S. K. (2007). Autotransporter structure reveals intra-barrel cleavage followed by conformational changes. *Nat Struct Mol Biol* **14**, 1214-20.